DOI: 10.2478/v10063-008-0005-8

ANNALES
UNIVERSITATIS MARIAE CURIE-SKŁODOWSKA
LUBLIN – POLONIA

VOL. LXIV, 4 SECTIO AA 2009

Argon adsorption studies of porous structure of nongraphitized carbon blacks♣

L. Gardner and M. Jaroniec
Department of Chemistry, Kent State University, Kent, OH 44-242, USA,
e-mail: jaroniec@kent.edu

Structural properties of a series of commercial nongraphitized carbon blacks were studied by means of argon adsorption at 87 K and 77 K. The specific surface area of the samples was calculated using the standard BET method. The micropore volume and external surface area were both calculated by the α_s-plot method. Pore volume and adsorption energy distributions were calculated numerically by using the regularization method. The above mentioned quantities obtained from argon adsorption isotherms were compared with those evaluated from nitrogen adsorption at 77 K.

1. INTRODUCTION

Carbon blacks, both graphitized and nongraphitized, are materials that have found wide applications in many different areas [1-3], because of their desirable features stemming from surface properties. Thus, the surface of carbon blacks has been extensively studied over the years using a wide variety of methods. For nongraphitized carbon blacks, recent surface studies have been conducted using thermogravimetry [4], mercury porosimetry [5], adsorption from solutions [6], and inverse gas chromatography [7,8].

Gas adsorption has long been known as a reliable method for characterization of porous solids [9-12]. For instance, adsorption of water vapor [13,14], benzene [15] and krypton [16] on nongraphitized carbon blacks have been studied. Nitrogen is the most common gas used to study any porous solid,

♣This article is dedicated to Professor Roman Leboda on the occasion of his 65th birthday

including nongraphitized carbon blacks [14, 16-19]. One gas that does not seem to have been used much in the study of nongraphitized carbon blacks is argon [20], even though it potentially has some advantages over nitrogen. For example, nitrogen has a quadrupole moment and may interact with functional groups on the carbon surface, which may make it more difficult to differentiate between surface and structural heterogeneity. Thus, it would be desirable to employ an adsorbate that interacts minimally with surface functional groups. To this end, argon would seem to be an attractive alternative to study the porous structures of carbons. Also, in the case of argon, the low-pressure data at 87 K may be better equilibrated and monolayer formation for argon at 87 K will take place at higher relative pressures than that for nitrogen at 77 K. Thus, argon at 87 K may be a better adsorptive to use in instruments that cannot measure very low relative pressures. Also, the BET surface areas calculated from nitrogen data are often inaccurate [21], whereas the BET surface areas from argon data are more reasonable. Liquid argon is three times as expensive as liquid nitrogen, so it would also be desirable if argon can be used to characterize the surfaces of nongraphitized carbon blacks at the liquid nitrogen temperature of 77 K.

This paper presents the results of a systematic study of a series of carbon blacks that involved measurement of argon adsorption isotherms at 87 K and 77 K. These isotherms were analyzed using the α_s–plot method and were used to calculate the pore size distributions, adsorption potential distributions and adsorption energy distributions. This analysis was compared with a parallel study performed earlier that used nitrogen as an adsorbate [22].

2. EXPERIMENTAL

Materials. A series of commercial nongraphitized Black Pearls carbon blacks labeled BP 120, BP 280, BP 460, BP 800, BP 1300 and BP 2000 was supplied by Cabot Corporation Special Blacks Division in Billerica Massachusetts. According to the manufacturer, the average size of primary particles ranges from 12 nm to 75 nm.

Measurements. Argon adsorption measurements were carried out at 87 K and 77 K using an ASAP 2010 static volumetric adsorption analyzer from Micromeritics in Norcross, Georgia. This automatic instrument is equipped with 1000, 10, and 1 Torr pressure transducers and was used to accurately measure argon adsorption data in a relative pressure range of 10^{-6}–10^{-7} to 0.99. High purity (99.999%) argon was used. Prior to the measurements, all samples were degassed under argon at 473 K for two hours.

Calculation Methods. The adsorption potential A is defined as the negative of the change in the Gibbs free energy of adsorption: $A = -\Delta G = RTln(p_0/p)$, where R is the universal gas constant, T is the absolute temperature, p_o is the saturation vapor pressure, and p is the equilibrium vapor pressure [10]. Then the adsorption potential distribution, or APD [10], was calculated by numerical differentiation of the adsorption isotherm: $X(A) = -d\Theta_t(A)/dA$, where $\Theta_t(A)$ is the total relative adsorption obtained by dividing the volume adsorbed by the BET monolayer capacity.

Adsorption energy distributions were calculated from submonolayer adsorption data by inverting the integral equation for the overall adsorption [10]:

$$\Theta_t(p) = \int_{\varepsilon_{min}}^{\varepsilon_{max}} \theta_l(p,\varepsilon)F(\varepsilon)d\varepsilon \quad (1)$$

where $\theta_l(p,\varepsilon)$ is the local adsorption isotherm for sites of the adsorption energy equal to ε, and $F(\varepsilon)$ is the distribution of the adsorption energy in the interval from ε_{min} to ε_{max}.

The local adsorption isotherm employed is the Fowler-Guggenheim isotherm [23], given by

$$\theta_l(p,\varepsilon) = \frac{K_L p \exp(z\omega\theta_l / k_B T)}{1 + K_L p \exp(z\omega\theta_l / k_B T)} \quad (2)$$

with

$$K_L = K_L^0(T)\exp(-\varepsilon / k_B T) \quad (3)$$

where K_L is the Langmurian constant for adsorption on sites of the energy ε. The pre-exponential factor K_L^0 can be expressed in terms of partition functions for an isolated molecule in the gas and surface phases. The parameter ω describes the energy of lateral interactions between two nearest neighbor molecules, while the parameter z gives the number of nearest neighbors. In the studies presented here, the INTEG program was used, which solves the above integral by the regularization method [24]. In this program, singular value decomposition is used on the matrix that represents the adsorption isotherm [25], and a patchwise topography was assumed. The number of nearest neighbors used was 2, and the interaction parameter $\omega z/k_B$ =118K was used [26].

Pore size distributions were calculated using the commercial program DFT plus from Micromeritics in Norcross, Georgia [27]. The α_s plots [28] were constructed by plotting the amount adsorbed versus the reduced adsorption α_s,

where $\alpha_s = v(p/p_o)/v(0.4)$ with $v(p/p_o)$ being the volume adsorbed at relative pressure p/p_o, $v(0.4)$ is the volume adsorbed at relative pressure 0.4, p_o is the saturation vapor pressure, and p is the equilibrium vapor pressure.

The specific surface area was calculated using the Brunauer-Emmett-Teller (BET) method [12], using adsorption data in the relative pressure range 0.05–0.14. For samples with mesopores and micropores, such as the nongraphitized carbon blacks presented here, total pore volume is the amount of gas adsorbed at the maximum relative pressure achieved during the measurement, converted to the equivalent liquid volume.

3. RESULTS AND DISCUSSION

Argon adsorption-desorption isotherms for Black Pearls carbons at 87 K and 77 K are shown in Figure 1. According to the IUPAC classification [29] the adsorption isotherms at 77 K are of type II for BP 120, 280 and 460; intermediate between types II and IV for BP 800 and 1300; and type I for BP 2000. The isotherms at 87 K are intermediate between types II and IV for BP 120, 280 and 460; of type IV for BP 800 and BP 1300, and intermediate between types I, II and IV in the case of BP 2000. The isotherms at 87 K also exhibit a hysteresis loop, which indicates that the capillary condensation is taking place in mesopores and macropores of size close to the mesopore range. It should be noted that in the discussion here, the IUPAC definition of pore size is being used [29], in which micropores are less than two nm wide, mesopores are between two and fifty nm wide, and macropores are greater than 50 nm. Hysteresis loops at 77 K are observed for BP 800 and BP 1300, whereas there is also some evidence of hysteresis for BP 120, 280, 460 and 2000, although hysteresis loops are not well-pronounced. In the case of argon adsorption at 87 K, the hysteresis loops for BP 120, 280, 460, and 2000 are narrow, and located at pressures close to the saturation vapor pressure, suggesting that the fraction of mesopores present may be low, while larger hysteresis loops for BP 800 and BP 1300 provide evidence of a larger fraction of mesopores.

For all the isotherms at 87 K, the amount adsorbed rises more steeply at higher relative pressures than that recorded at 77 K. This is due to the fact that argon will condense in larger pores at 87 K but will not condense in these pores at 77 K. Also, isotherms for BP 120, 280, 460 and 2000 do not level of at high relative pressures, which may be due to unrestricted monolayer-multilayer adsorption on the surface of large mesopores and macropores.

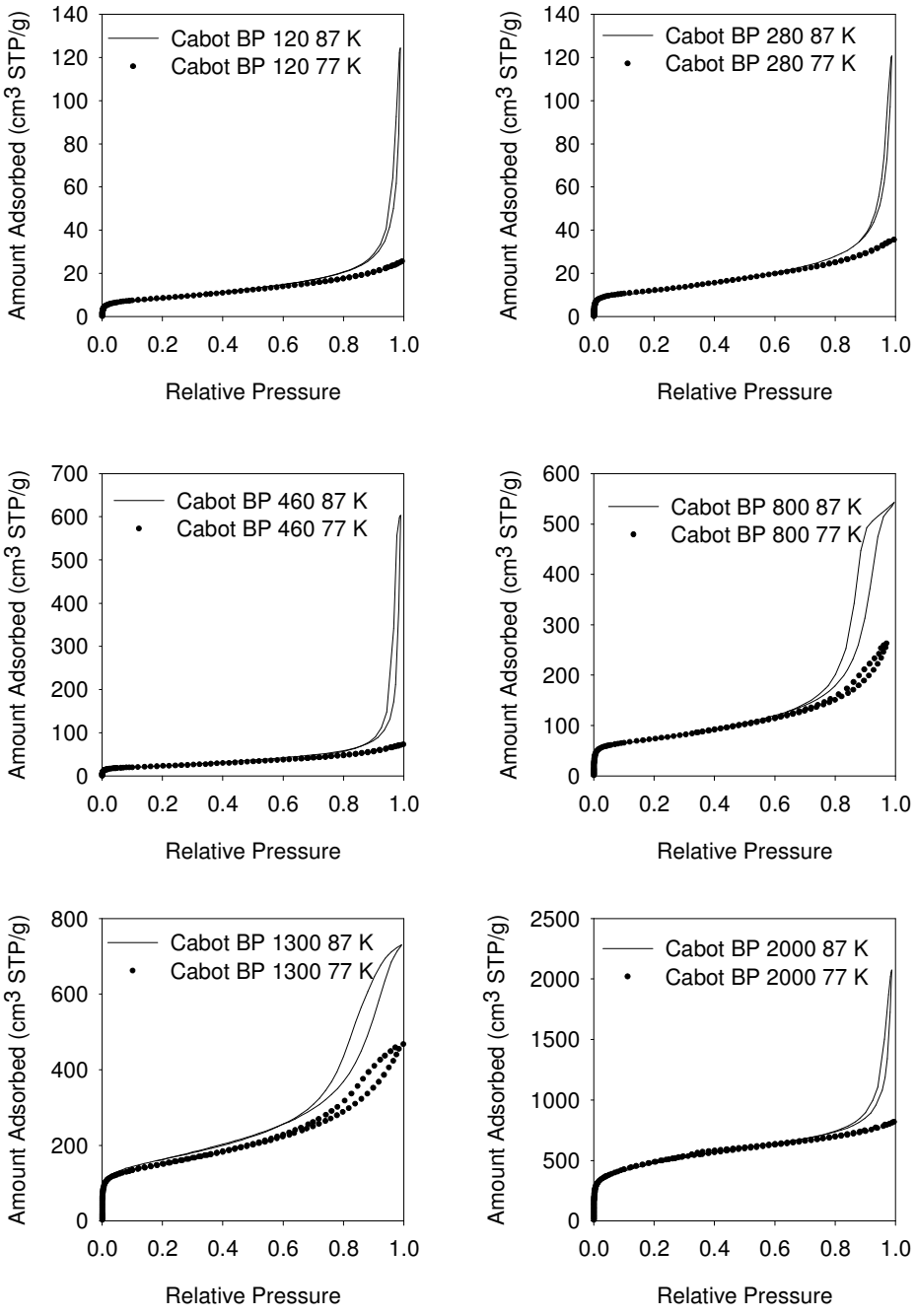

Fig. 1. Argon adsorption-desorption isotherms at 87 K and 77 K plotted in a linear scale.

At lower relative pressures the amount adsorbed at 87 K and 77 K is similar until a relative pressure of about 0.5 for all samples, and only BP 1300 exhibits some deviation from this trend. The hysteresis loop closes at a relative pressure of about 0.7 for BP 800 and 1300 and a relative pressure of about 0.9 for the other carbons. Capillary condensation begins at lower relative pressures in smaller pores, providing further evidence that BP 800 and 1300 have a larger fraction of mesopores than the other samples. The BP 120, 280, 460 and 2000 carbons do not exhibit any pronounced adsorption-desorption hysteresis at 77 K, whereas BP 800 and 1300 exhibit hysteresis loops somewhat similar to type H1. At 87 K, these samples exhibit H1 hysteresis loops, whereas the other samples also exhibit hysteresis loops similar to type H1.

Figure 2 shows the isotherms from Figure 1, this time using a logarithmic scale for relative pressure to better show adsorption behavior at low pressures. The amount adsorbed at low pressures is quite comparable at both temperatures. Monolayer formation at relative pressures between 10^{-3} and 10^{-2} can be seen for all samples. BP 800, 1300 and 2000 exhibit pronounced adsorption at relative pressures below 10^{-5}, suggesting the presence of microporosity, with BP 2000 having the highest fraction of micropores.

The low pressure isotherms for argon adsorption at 87 K and 77 K are similar; almost equal amounts adsorb at low pressures for these two systems. However, there are differences in when adsorption begins. For the BP 120, 460, and 800 samples argon begins adsorbing at lower relative pressure at 77 K than at 87 K; however, for the BP 800, 1300 and 2000 carbons, adsorption starts at higher relative pressures. The latter carbons have micropores, and it is possible that argon is not equilibrating as well in the pores of this size at 77 K.

Adsorption potential distributions (APDs) for the BP carbons studied at 87 K and 77 K are shown in Figure 3. They all have a single, broad peak of about the same width and located at about the same position, between 4–5 kJ/mol. This peak is associated with monolayer formation on the pore walls and on the external surface. The broadness of this peak provides evidence that the BP carbons have significant surface heterogeneity [22,30].

The isotherms for BP 1300 and BP 2000 suggest that these carbons have a significant number of micropores. If this is true, we might expect the APD curves to exhibit more than one peak. If the micropores are small enough, there would be one additional peak at higher values of the adsorption potential, due to micropore filling. However, the APD curves for BP 1300 and BP 2000 show only one broader peak with tailing in direction to higher adsorption potentials. This may be due to their very large external surface area, shown in Tables 1 and 2, and the presence of larger micropores. Such a large surface area is expected to produce a broad monolayer formation peak that may mask the micropore filling peak.

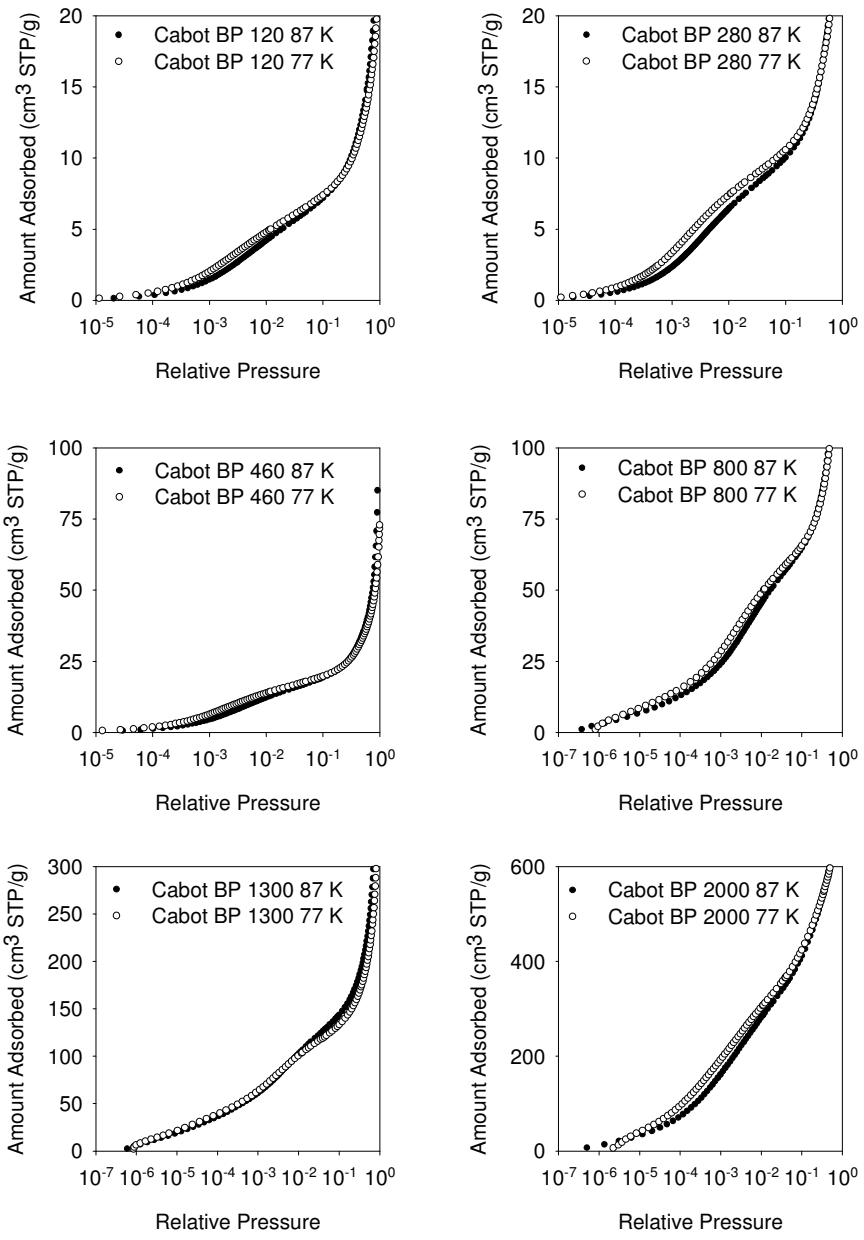

Fig. 2. Argon adsorption-desorption isotherms at 87 K and 77 K plotted using the logarithmic scale of relative pressure.

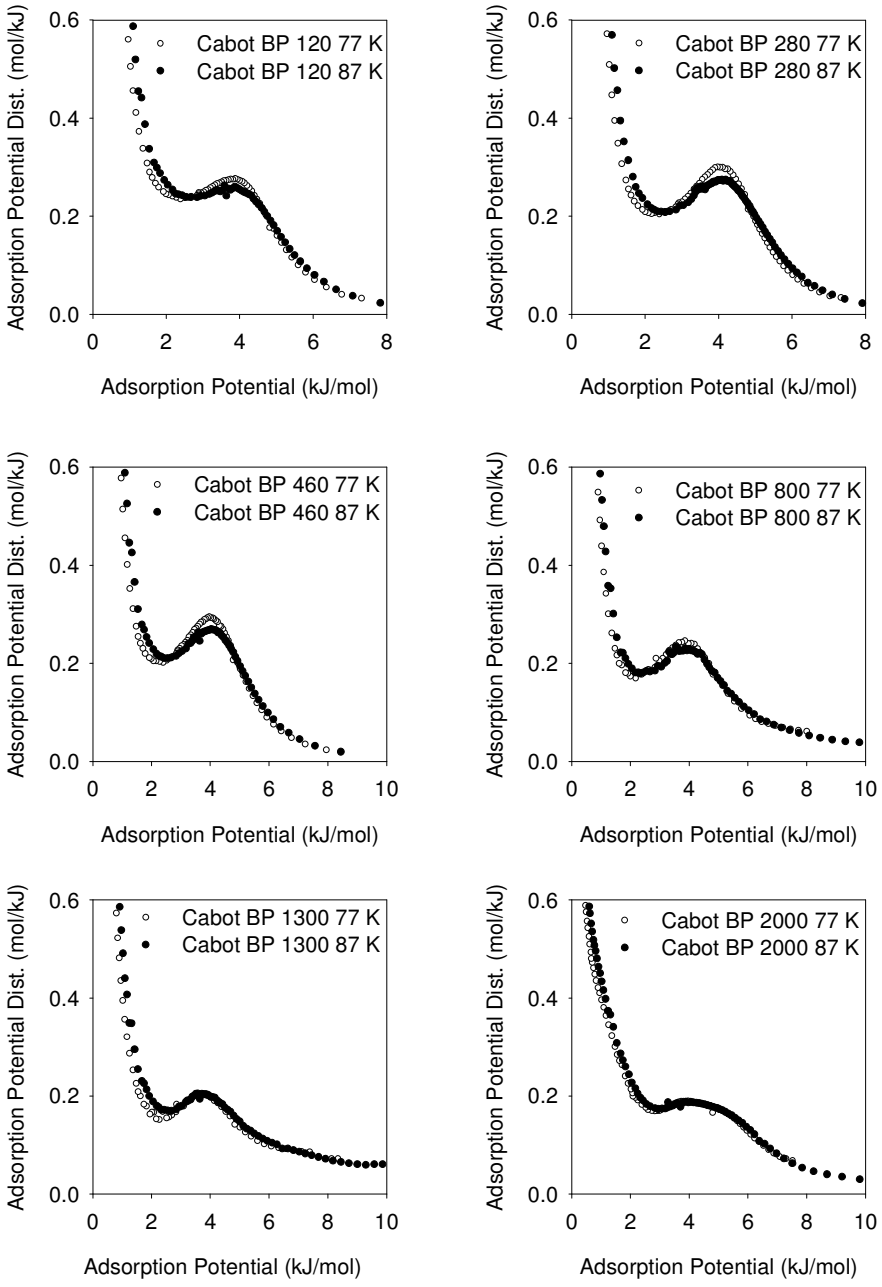

Fig. 3. Adsorption potential distributions for the BP carbon samples studied at 87 K and 77 K.

Tab. 1. Surface and structural parameters for the carbon blacks studied at 87 K.*

Sample	S_{BET} (m^2/g)	S_{APD} (m^2/g)	S_{DFT} (m^2/g)	S_{ex} (m^2/g)	V_{mi} (cm^3/g)	V_t (cm^3/g)
BP 120	27	20	21	28	0	0.16
BP 280	37	30	29	38	0	0.15
BP 460	71	58	57	76	0	0.76
BP 800	230	212	210	202	0.01	0.68
BP 1300	510	440	480	400	0.05	0.93
BP 2000	1500	1100	1230	630	0.38	2.61

* S_{BET} – BET specific surface area, S_{APD} – specific surface area evaluated using the minimum on the adsorption potential distribution [31], S_{DFT} – specific surface area evaluated using using the DFT software supplied by Micromeritics Co., S_{ex} – external surface area obtained by the α_s–plot method [32,33], V_{mi} – micropore volume obtained by the α_s–plot method [32,33], and V_t – single-point pore volume obtained from adsorption at the relative pressure of 0.98 (note that for the type II isotherms, which are observed for macroporous solids, argon at 87 K do not condense in macropores; thus, this volume represents rather the volume of adsorbed film on the pore walls).

Tab. 2. Surface and structural parameters for the carbon blacks studied at 77 K.

Sample	S_{BET} (m^2/g)	S_{APD} (m^2/g)	S_{ex} (m^2/g)	V_{mi} (cm^3/g)	V_t* (cm^3/g)
BP 120	27	21	26	0	0.03
BP 280	38	33	38	0	0.04
BP 460	71	60	73	0	0.08
BP 800	230	218	196	0.01	0.29
BP 1300	500	440	360	0.05	0.57
BP 2000	1550	1140	720	0.38	1.04

* The pore volumes at 77 K are smaller than those at 87 K because argon at 77 K does not condense at mesopores exceding 15 nm.

Surface and structural parameters for the BP carbons studied are shown in Table 1 for adsorption at 87 K and Table 2 for adsorption at 77 K. The external surface area and the micropore volume were determined by the α_s–plot method [32,33]; the BP 280 carbon was used as the reference nonporous carbon surface [34]. The specific surface areas were calculated by three different methods (see information under Table 1). Since there is a corresponding increase in the micropore volume and total pore volume, the increase in the surface area can be attributed to an increase in porosity. The surface areas calculated by using the

BET method differ from those obtained with the help of the adsorption potential distributions (S_{APD}) [31] and the DFT method (S_{DFT}) [27]; this difference becomes significant for high surface area samples. At 87 K, S_{APD} and S_{DFT} agree quite well for all samples except slightly larger difference for BP 2000.

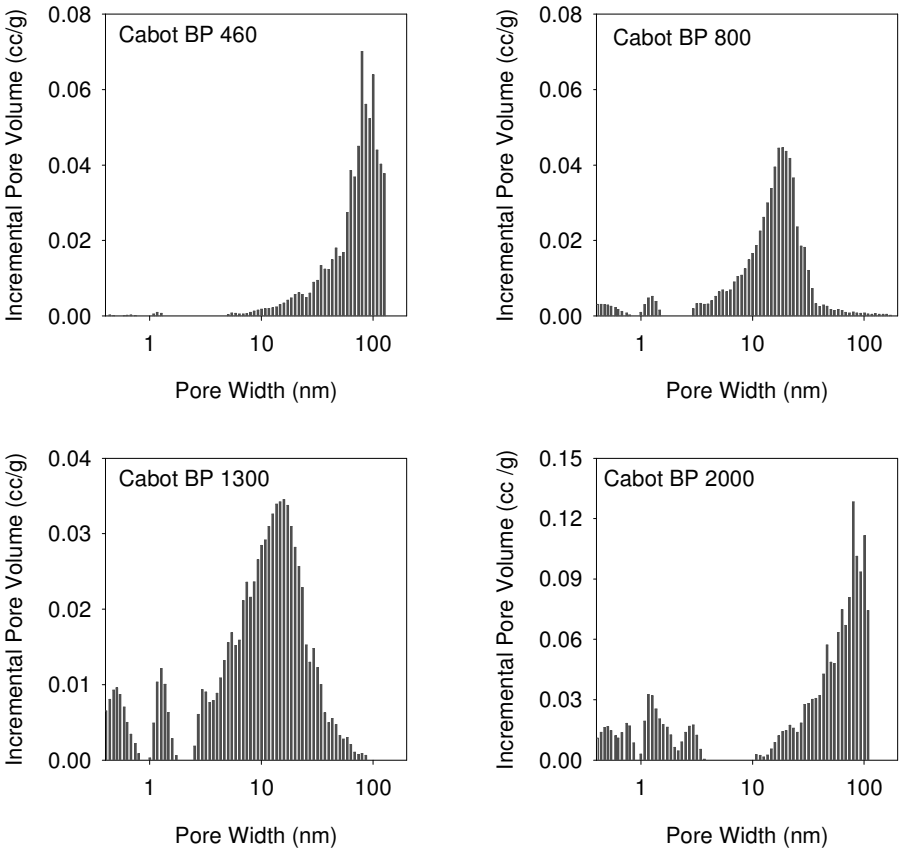

Fig. 4. Pore size distributions for porous BP carbon sampels.

Shown in Figure 4 are pore size distributions (PSDs) obtained from argon adsorption at 87 K for the BP carbons with larger porosity only, i.e. BP 460, 800, 1300 and 2000. The PSD curves were not calculated for BP 120 and 280 because these samples are rather nonporous with some large macropores only. Argon data at 77 K were not analyzed because at this temperature argon does not condense in larger mesopores. BP 800 and BP 1300 exhibit larger porosity in the range of mesopores (PSD peak located around 10–20 nm), while BP 460 and 2000 possess larger mesopores and small macropores (PSD peak closer to 100 nm).

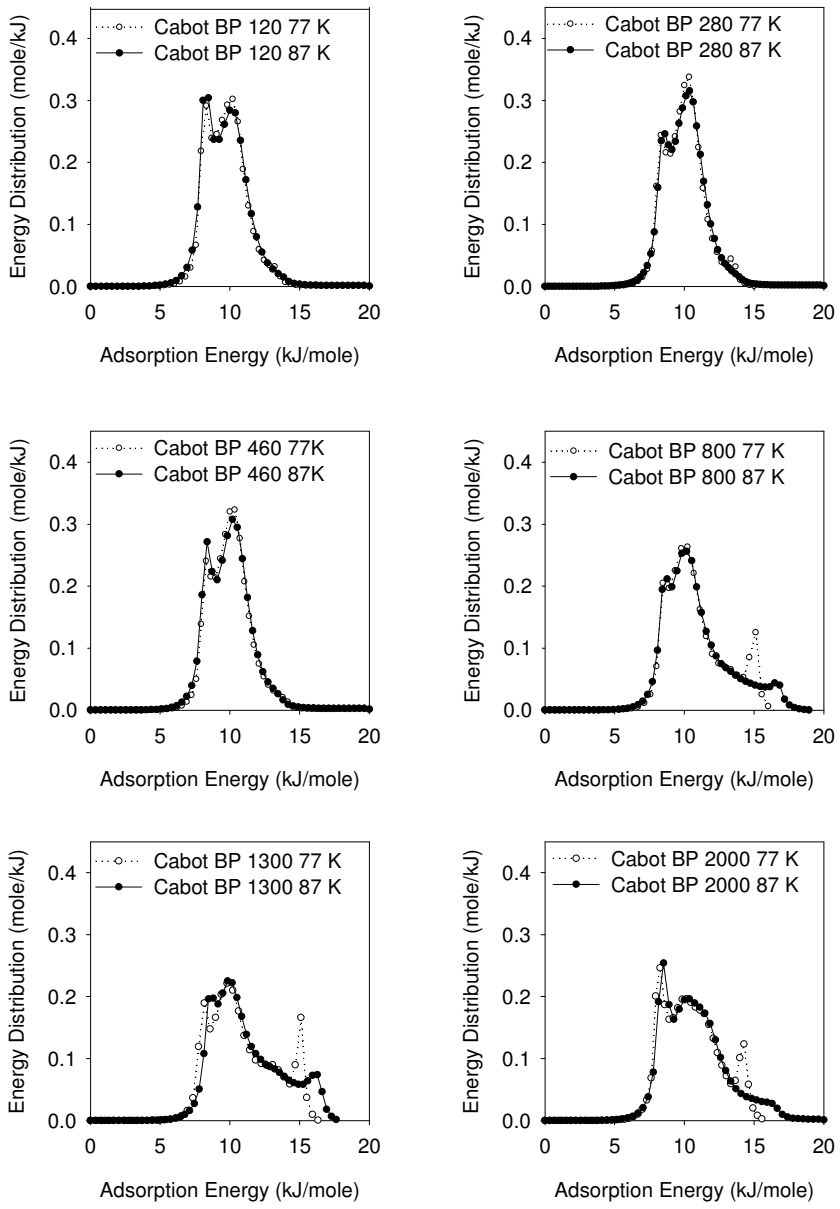

Fig. 5. Adsorption energy distributions for the BP carbons studied.

BP 1300 is more porous than BP 800 but both exhibit some microporosity. BP 2000 is the most porous sample among the BP carbons studied, and has a noticeable gap in the mesopore region. The increased mesoporosity of BP 800 and BP 1300 leads to broader hysteresis loops in their isotherms. Finally, the lack of appreciable mesoporosity leads to a narrow hysteresis loop for BP 2000, and indicates that the macropores present adsorb argon by a mechanism similar to a flat surface, with only a small contribution from capillary condensation.

Adsorption energy distributions (AEDs) for the BP carbons studied at 87 K and 77 K are shown in Figure 5. All the curves show two not well-resolved peaks at ~8 kJ/mol and 11 kJ/mol. For BP 120, the peaks are roughly equal in magnitude. For BP 280 and BP 460, the peak at 11 kJ/mol is considerably larger, while the shapes of the distributions are being similar. For BP 800 and BP 1300, the peaks are both smaller, with the peak at 11 kJ/mol once again being larger. BP 2000 shows the reverse of the other samples, with the peak at 8 kJ/mol being much larger than the peak at 11 kJ/mol. For BP 120, 280 and 1300, the shapes of the distributions at 77 K and 87 K are almost the same. However, the other three samples all show an extra peak, corresponding to energy of about 15 kJ/mol at 77 K and about 17 kJ/mol at 87 K. In all three of these samples, the third peak at 77 K is much larger than the peak at 87 K.

The high adsorption energies correspond to adsorption at low relative pressures. So the peaks at 8 and 11 kJ/mol can be attributed to monolayer formation on the mesopore and macropore surface. For solids that are macroporous and/or mesoporous such as BP 120, 280 and 460, the AED reflects the surface heterogeneity [32]. Thus, the fact that the AED curves for BP 280 and 460 (Figure 5) are similar indicates that their surface heterogeneities are similar. On the other hand, the AED curve for BP 120 has a slightly different shape than BP 280 and 460, so its surface heterogeneity is somewhat different. The PSDs in Figure 4 show that BP 800, 1300, and 2000 have micropores, so the AEDs for these carbons reflect both structural and surface heterogeneities, and it is difficult to separate the two. But it might be possible by comparing the AED and PSD curves. For example, the onset of microporosity on the PSD curves for BP 800, 1300 and 200 correspond to a new feature on the AED curves, namely a third peak at ~15 kJ/mol. This suggests that this third peak in the AEDs is due to the filling of micropores. This peak occurs at an adsorption energy that corresponds to lower relative pressures than the onset of monolayer formation, which lends further credence to the above suggestion. In addition, the range of micropores shown on the PSD curves is quite narrow, which resulted in a narrow third peak on the AED curevs.

When argon adsorption isotherms at 87 K are compared with previous published nitrogen adsorption isotherms at 77 K [22], it is found that the nitrogen isotherms show the same trends as the argon isotherms in terms of the

shape of the isotherm, the amount adsorbed, and the types of hysteresis loops that are found as the BP series progresses. Thus it is seen that argon adsorption isotherms at 87 K give analogous information about the porosity of nongraphitized carbon blacks as nitrogen adsorption does.

4. CONCLUSIONS

Argon adsorption-desorption isotherms were measured on a series of six nongraphitized carbon blacks at 87 K and 77 K. The isotherms show greater adsorption of argon at higher relative pressures at 87 K than at 77 K due to the lack of argon condensation in larger mesopores at 77 K. The low-pressure isotherms give the first indication that BP 1300 and BP 2000 have significant microporosity. Adsorption energy distributions show some small differences in energetic heterogeneity of BP 120, BP 280 and BP 460, even though their isotherms are similar. The high energy part of these distributions provides evidence about microprosity, which is reflected by a small peak at ~15 kJ/mol. A comparison of argon isotherms at 87 K with an earlier study done for nitrogen at 77 K indicates that both adsorbates seem to able to detect the same trends in the surface properties and porosity of these nongraphitized carbon blacks. The use of argon can be beneficial for carbons with small micropores.

Acknowledgements. The authors would like to express their best wishes to Professor R. Leboda on the occasion of his 65th birthday anniversary. Also, they would like to thank Prof. Michal Kruk for valuable discussions.

5. REFERENCES

[1] J. Donnet, R. C. Bansal, M. Wang (eds), *Carbon Black, Science and Technology*, Marcel Dekker, New York, 1993.
[2] R. Leboda, A. Łodyga, A. Gierak, *Mater. Chem. Phys.,* 51, 216 (1997).
[3] R. Leboda, A. Łodyga, B. Charmas, *Mater. Chem. Phys.,* 55, 1 (1998).
[4] Z. J. Li, M. Jaroniec, *J. Colloid Interface Sci.,* 210, 200 (1999).
[5] R. Pirard, B. Sahouli, S. Blacher, J.P. Pirard. *J. Colloid Interface Sci.,* 217, 216 (1999).
[6] C. M. Gonzalez-Garcia, M. L. Gonzalez-Martin, V. Gomez, Serrano, J. M. Bruque, and L. Labajos-Broncano, *Langmuir,* 16, 3950 (2000).
[7] H. Darmstadt, N. Z. Cao, D. M. Pantea, C. Roy, L. Summchen, U. Roland, J. B. Donnet, T. K. Wang, C. H. Peng, P. J. Donnelly, *Rubber Chem. Tech.,* 73, 293 (2000).
[8] M. J. Wang, S. Wolff, B. Freund, *Rubber Chem. Tech.,* 67, 27 (1994).
[9] S. J. Gregg, K. S. W. Sing, *Adsorption, Surface Area and Porosity*, London, Academic Press, 1982.
[10] M. Jaroniec, R. Madey, *Physical Adsorption on Heterogeneous Solids,* Amsterdam, Elseveier, 1988.
[11] W. Rudzinski, D. H. Everett, *Adsorption of Gases on Heterogeneous Solid Surfaces,* London, Academic Press, 1991.

[12] F. Rouquerol, J. Rouquerol, K. S. W. Sing, *Adsorption by Powders and Porous Solids*, London, Academic Press, 1999.
[13] A. R. Chughtai, G. R. Williams, M. M .O. Atteya, N. J. Miller, D. M. Smith, *Atmos. Environ.,* 33**,** 2679 (1999).
[14] J. Choma, W. Burakiewicz-Mortka, M. Jaroniec, Z. Li, J. Klinik, *J. Colloid Interface Sci.*, 214, 438 (1999).
[15] P. J. M. Carrott, M. M. L. R. Carrott, I. P. P. Cansado, J. M. V. Nabais, *Carbon,* 38, 465 (2000).
[16] H. Naono, M. Shimoda, N. Morita, M. Hakuman, K. Nakai, S. Kondo, *Langmuir,* 13, 1297 (1997).
[17] C. Roy, H. Darmstadt, *Plast. Rub. Composite Proc.,* 27, 341 (1998).
[18] R. H. Bradley, I. Sutherland, E. Sheng, *J. Colloid Interface Sci.,* 179**,** 561 (1996).
[19] B. Sahouli, S. Blacher, F. Brouers, L. Chahed, *Can. J. Phys.*. **77,** 653 (1999).
[20] A. Schroder, M. Kluppel, R.H. Schuster, *Kaut. Gummi Kunstst.,* 52**,** 814 (1999).
[21] F. Rodriguez-Reinoso, J. M. Martín-Martínez, B. McEnaney, *Carbon,* 27, 297 (1989).
[22] M. Kruk, M. Jaroniec, Y. Bereznitski, *J. Colloid. Interface Sci.,* 182, 282 (1996).
[23] R. H. Fowler, E. A. Guggenheim, *Statistical Thermodynamics,* London, Cambridge University Press (1949).
[24] M.v. Szombathely, P. Brauer, M.Jaroniec, *J. Comp. Chem.,* 13, 17 (1992).
[25] W. H. Press, S. A. Teukolsky, W. T. Vetterling, B. P. Flannery, *Numerical Recipes in C,* Cambridge: Cambridge University Press, 1992.
[26] P. I. Ravikovitch, A. Vishnyakov, R. Russo, A. V. Neimark, *Langmuir,* 16, 2311 (2000).
[27] J. P. Olivier, W. B. Conklin, M.v. Szombathely *Stud. Surf. Sci. Catal.,* 87, 81 (1994).
[28] K. S. W. Sing, in *Surface Area Determination,* D. H. Everett, R. H. Ottewill (eds), Butterworths, London, 1970, p. 25.
[29] K. S. W. Sing, D. H. Everett, R. A. W. Haul, L. Moscou, R. A. Pierotti, J. Rouquerol, T. Siemieniewska, *Pure Appl. Chem.,* 57, 603 (1985).
[30] M. Jaroniec, M. Kruk, J. Choma, in *Characterization of Porous Solids IV*, B. McEnaney, T. J. Mays, J. Rouquerol, F. Rodrigues-Reinoso, K. S. W. Sing, K. K. Unger (eds), Royal Society of Chemistry, Cambridge, 1997, p. 163.
[31] M. Kruk, M. Jaroniec, K. P. Gadkaree, *Langmuir,* 15**,** 1442 (1999).
[32] M. Jaroniec, in *Access in Nanoporous Materials,* T. J. Pinnavia, M. F. Thorpe (eds), Plenum, New York , 1995, p. 255.
[33] M. Kruk , M. Jaroniec, *Chem. Mater.* 13, 3169 (2001).
[34] M. Kruk, M. Jaroniec, K. P. Gadkaree, *J. Colloid Interface Sci.,* 192, 250**,** (1997).

CURRICULUM VITAE

Mieczysław Jaroniec was born in 1949 in Okrzeja, Poland. He studied chemistry at M. Curie-Sklodowska University (UMCS) in Lublin, Poland, between 1967 and 1972. After graduating with honors in 1972, he was employed at UMCS and joined the Department of Physical Chemistry, and in 1975, he moved to the newly created Department of Theoretical Chemistry. He defended his PhD dissertation under the guidance of Professor W. Rudzinski in 1976. In 1985 and 1989 he received both professor titles. In 1991, he moved to Kent State University, Ohio, and has been a professor there since.

Professor Jaroniec has had several visiting appointments, including Georgetown University, USA (1984–1985), McMaster University, Canada (1985–1986), Kent State University, USA (1987, 1988–1989), and Chiba University, Japan (1997). He has published over 850 papers in the area of adsorption, chromatography, thermal analysis, nanoporous materials, and self-assembled ordered mesoporous materials, and has been co-chairman of four international symposia on nanoporous materials held in Canada in 2000, 2002, 2005 and 2008. In addition, he has co-edited three volumes of Nanoporous Materials, published in the Elsevier series of *Studies in Surface Science and Catalysis*. The forth volume of "Nanoporous Materials" has been published by World Sci. Publishers in 2008. Also, he co-edited a special issue of *Chemistry Materials* devoted to templated materials (Feb 2008), edited a special volume of the *Journal of Liquid Chromatography* (1996), dedicated to the synthesis, characterization, and application of chemically bonded phases, and co-authored a book Physical Adsorption on Heterogeneous Solids, published by Elsevier in 1988. Professor Jaroniec has served and is currently serving on the editorial boards of *Adsorption*, *Adsorption Science & Technology*, *Chemistry Materials, Journal of Liquid Chromatography*, *Journal of Porous Materials*, *Dekker Encyclopedia of Nanoscience and Nanotechnology*, *Journal of Colloid and Interfacial Science*, *Thin Solid Films*, and *Heterogeneous Chemistry Reviews*. Among the numerous awards he has received, he cherishes especially an Honorary Professor title of M. Curie-Skłodowska University, Poland (2005), doctor honoris causa from Copernicus University, Poland (2009) and a Distinguished Scholar Award from Kent State University (2002).

Research interests and activities of Professor Jaroniec revolve primarily around interdisciplinary topics of interfacial chemistry, chemical separations, and chemistry of materials, especially physical adsorption at the gas/solid and liquid/solid interfaces, gas and liquid chromatography, the synthesis, modification, and characterization of adsorbents, chromatographic packings, catalysts, and most recently, ordered nanoporous materials. During his employment at Kent State University, he has established a vigorous research program in the area of advanced nanomaterials, such as surfactant- and polymer-templated ordered mesoporous silicas, organosilicas, and carbons.